

# Torque terms and grain-boundary energy measurement

BARBARA K. HODGSON\*, H. MYKURA  
*Physics Department, University of Warwick, Coventry, UK*

The surface-energy anisotropy of nickel at 1000°C has been re-determined from measurements of the shape of twin boundary-surface intersections. The measurements were used to correct measurements of the energy of seventy-one individual grain boundaries made on the same specimen, for torque-term effects. The average correction to individual grain boundaries was 20%, but the effect of the torque-term corrections on the average value of the grain boundary/surface-energy ratio was less than the experimental error in the ratio.

## 1. Introduction

The usual method of determining grain-boundary energy, in polycrystalline materials, is to measure the grain-boundary energy/surface-energy ratio,  $\gamma_b/\gamma_s$ , and to use a value of the surface energy,  $\gamma_s$ , obtained from "zero-creep" measurements to obtain an absolute value of  $\gamma_b$  (see Hondros [1] who refers to the earlier literature). This method works quite well if the variation of  $\gamma_b$  and  $\gamma_s$  with crystallographic orientation are negligibly small. In that case the local equilibrium at the intersection of a grain boundary with a surface gives the usual "surface-tension" equilibrium (assuming the grain boundary is normal to the surface)

$$\gamma_b = \gamma_s \sin \theta_1 + \gamma_s \sin \theta_2 = 2\gamma_s \sin \theta \quad (1)$$

(if  $\theta_1 = \theta_2$ )

or

$$\gamma_b/\gamma_s = 2 \sin \theta = 2 \cos (D/2). \quad (2)$$

The determination of the  $\gamma_b/\gamma_s$  ratio is then reduced to a simple measurement of the dihedral angle  $D$  (or the angles  $\theta$ ) on a specimen which has been equilibrated at the temperature at which the  $\gamma_b/\gamma_s$  ratio is to be measured (Fig. 1a).

In practice, however, the surface energy varies significantly with surface orientation and the grain-boundary energy depends both on misorientation across the boundary and on the orientation of the plane of the boundary for a given misorientation. In the general case, therefore, the simple surface-tension formula has to be

replaced by the more general Herring [2] equilibrium formula

$$\sum_{i=1}^3 \gamma_i \mathbf{t}_i + \left( \frac{\partial \gamma}{\partial \alpha} \right)_i \mathbf{n}_i = 0 \quad (3)$$

( $\mathbf{t}_i$  is a unit vector in the plane of the  $i$ th interface, normal to the line of intersection of the interfaces;  $\mathbf{l}$  is a unit vector along the line of intersection and  $\mathbf{n}_i = \mathbf{l} \times \mathbf{t}_i$ ). For the grain boundary/surface intersection the equilibrium condition (ignoring the grain-boundary torque term) gives the grain-boundary energy as:

$$\gamma_B = \gamma_Q \sin \theta_Q + \gamma_R \sin \theta_R - \frac{\partial \gamma_Q}{\partial \alpha} \cos \theta_Q - \frac{\partial \gamma_R}{\partial \beta} \cos \theta_R \quad (4)$$

(We use the following suffix notation for surface and interface energies: average value – lower case suffix, e.g.  $\gamma_b$ ; specific value for a particular orientation – capital suffix, e.g.  $\gamma_B$  for a grain boundary;  $\gamma_Q, \gamma_R, \gamma_S$  for surfaces. The angles in the definitions of the orientation derivatives – the Herring "torque terms" – are measured in radians about  $\mathbf{l}$ .)

To determine the  $\gamma_b/\gamma_s$  ratio in the general case one needs to know not merely the angles at the intersection and the crystal orientations, but also the variation of  $\gamma_s$  with surface orientation and the variation of  $\gamma_B$  with the orientation of the

\*Now at the Department of Physics, Liverpool Polytechnic, Liverpool, UK.

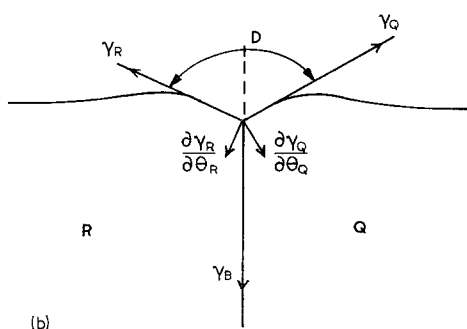
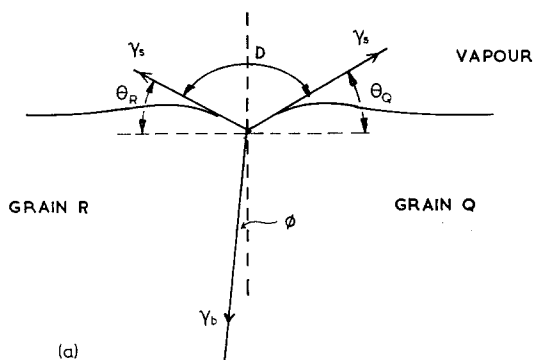


Figure 1 (a) Equilibrium configuration of the intersection of grain boundary with surface:  $\gamma_b/\gamma_s = 2 \cos D/2$ , assuming grain boundary vertical, i.e.  $\phi = 0$ . (b) System of equivalent forces acting at grain boundary-surface intersection according to Herring. (Grain boundary torque term omitted.)

$$\gamma_B = (\gamma_R + \gamma_Q) \cos \frac{D}{2} - \left( \frac{\partial \gamma_R}{\partial \theta_R} + \frac{\partial \gamma_Q}{\partial \theta_Q} \right) \sin \frac{D}{2}$$

(again assuming the grain boundary is vertical).

plane of the boundary (Fig. 1b). (The misorientation across a boundary is fixed for a given pair of crystals during the time in which local equilibrium is achieved at the grain boundary-surface intersection.) As it would be extremely laborious to determine all these parameters for a number of individual boundaries, the usual approach has been to rely on the fact that, for a large number of random boundaries, the terms in  $\partial\gamma/\partial\alpha$  are equally likely to be positive or negative and therefore they should not affect the average of a large number of  $\gamma_B/\gamma_S$  ratio measurements, provided there is no marked preferred orientation in the specimens used.

Individual values of the  $\gamma_B/\gamma_S$  ratio obtained using the simple formula (Equation 2) can be seriously in error and the spread about the mean value of a number of individual measurements of  $\gamma_B/\gamma_S$ , using the simple formula, is large (see below). We have therefore decided to investigate one set of  $\gamma_B/\gamma_S$  ratio measurements in detail, determining the individual crystal orientations for a large number of boundaries, and to determine the orientation dependence of the surface energy for that specimen. Corrections for the surface-torque terms can then be made using Equation 4 and the effect of torque terms on the individual ratios and on the mean  $\gamma_b/\gamma_s$  value for a large number of boundaries can be assessed.

## 2. The experimental techniques

The experiments were done using "Specpure" nickel sheet, 250  $\mu\text{m}$  thick, obtained from Johnson, Matthey & Co. The specimen was annealed in a vacuum of  $5 \times 10^{-7}$  Torr, supported in an alumina crucible, with a "Specpure" nickel lid to prevent net evaporation. There was an initial anneal of several hours at 1370°C, to produce a near-stable grain size much larger than the sheet thickness. This was followed by 144 h at 1000°C to obtain local equilibrium, by surface diffusion, at the intersection with the surface of grain boundaries (Fig. 1) and twin boundaries (Fig. 2). These high-temperature equilibrium shapes were then "quenched-in" by cooling to room temperature and were measured using interference microscopy. Most grains were multiply twinned so that grain orientations could be obtained by the twin-trace technique [3].

Interferograms of forty-four pairs of twin boundary-surface intersections for pairs of twins of known orientations were analysed to give the variation of torque terms with orientation, using the method described by Mykura [4]. Integration of these torque-term curves then gave the varia-

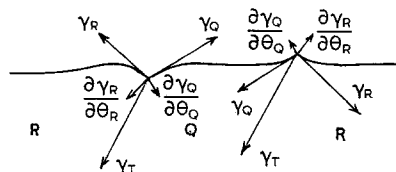


Figure 2 Equilibrium configuration of intersection of a pair of twin boundaries with the surface, showing directions of equivalent forces, from which the torque terms were evaluated (after [4]).

tion of surface-free energy with orientation. In this analysis, the simplifying assumption was made that torque terms near (111) and near (100) are due to conical cusps in the  $\gamma$ -plot, centred on these low index directions.

Interferograms were measured for seventy-one grain-boundary grooves, for which the orientations of both crystals forming the boundary were known. These measurements gave directly an apparent grain-boundary energy from Equation 2, ignoring torque terms and assuming the boundary was vertical. Also, using the known crystal orientation and the measured dihedral angle, the surface orientation at the root of the grain-boundary groove was obtained for each crystal. This orientation differs typically by 10 to 15° from the mean surface orientation of the crystal. The rotation of the surface orientation and the direction of the surface-torque term acting at the groove root were determined, using a stereographic net, from the direction of the boundary. The result of the measurements of torque terms from twin-boundary intersections (described above) then enabled the magnitude and sign of the surface-torque terms and the actual values of  $\gamma_s$  at the groove root to be evaluated. If it is assumed that the maximum torque  $(\partial\gamma_s/\partial\alpha)_{\max}$  of a surface acts towards a low index pole, the torque acting at the groove root is  $(\partial\gamma_s/\partial\alpha)_{\max} \cos \psi$ , where  $\psi$  is the angle between the axes of rotation of the actual and maximum-torque terms (Fig 3). The vertical

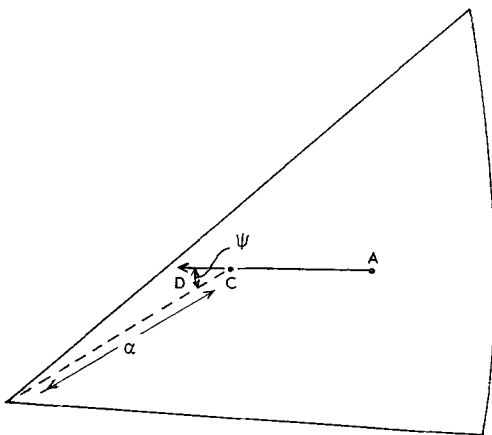


Figure 3 Stereographic representation of surface orientation at groove root and direction of the surface-torque term. A – general surface orientation, C – surface orientation at groove root, CD – direction of rotation of surface normal.

component of this torque term was then used in Equation 4 to correct the apparent grain-boundary energy.

This procedure gives a corrected grain-boundary energy which takes account of the two individual surface energies and the surface-energy torque terms. It is however based on the assumption that the grain boundary runs perpendicular to the general specimen surface and that the grain-boundary torque terms are negligible. The contribution of any horizontal component of  $\gamma_B$  is not really significant provided  $\phi \leq 5^\circ$  (Fig. 1a). Possible inclination of the grain boundary to the surface could be checked approximately by comparing the grain-boundary network on the front and back of the specimen, but this check still relies on the assumption that the boundaries are flat. Both grain-boundary torque terms and grain-boundary inclination will contribute some residual error to the mean  $\gamma_B/\gamma_s$  ratio.

### 3. Results and conclusions

The values of the torque terms near (111) and (100) are shown in Fig. 4 and the surface-energy anisotropy deduced from these is given in Fig. 5. It can be seen that, except within 5° of the (111) pole and 10° of the (100) pole, the surface anisotropy is < 2%. Very few orientations occur which are close to the poles and, except in these cases, correcting for the actual value of the surface energy makes negligible difference to the  $\gamma_B/\gamma_s$  ratios. Consequently, for most orientations an average value of  $\gamma_s$  was used introducing an error of not more than 2% in the  $\gamma_b/\gamma_s$  ratios.

For a typical boundary (orientation given in Fig. 6) the uncorrected value of  $\gamma_B/\gamma_s$  was 0.284. Torque term corrections in this case were  $(1/\gamma_s)(\partial\gamma_Q/\partial\theta_Q) = -0.120 \text{ rad}^{-1}$  and  $(1/\gamma_s)(\partial\gamma_R/\partial\theta_R) = +0.022 \text{ rad}^{-1}$  so that the corrected value of  $\gamma_B/\gamma_s$  was 0.382. The histogram for uncorrected  $\gamma_B/\gamma_s$  values is given in Fig. 7a and for corrected values in Fig. 7b. The average correction,

$$\left| \sum_2 \left( \frac{1}{\gamma_s} \frac{\partial\gamma}{\partial\theta} \sin \frac{D}{2} \right) \right|$$

was  $0.075 \text{ rad}^{-1}$  though in extreme cases it was up to  $0.22 \text{ rad}^{-1}$ .

It will be seen that while the surface torque terms do narrow the spread of values of individual  $\gamma_B/\gamma_s$  ratios, a substantial spread remains. Part of this spread is the genuine variation of

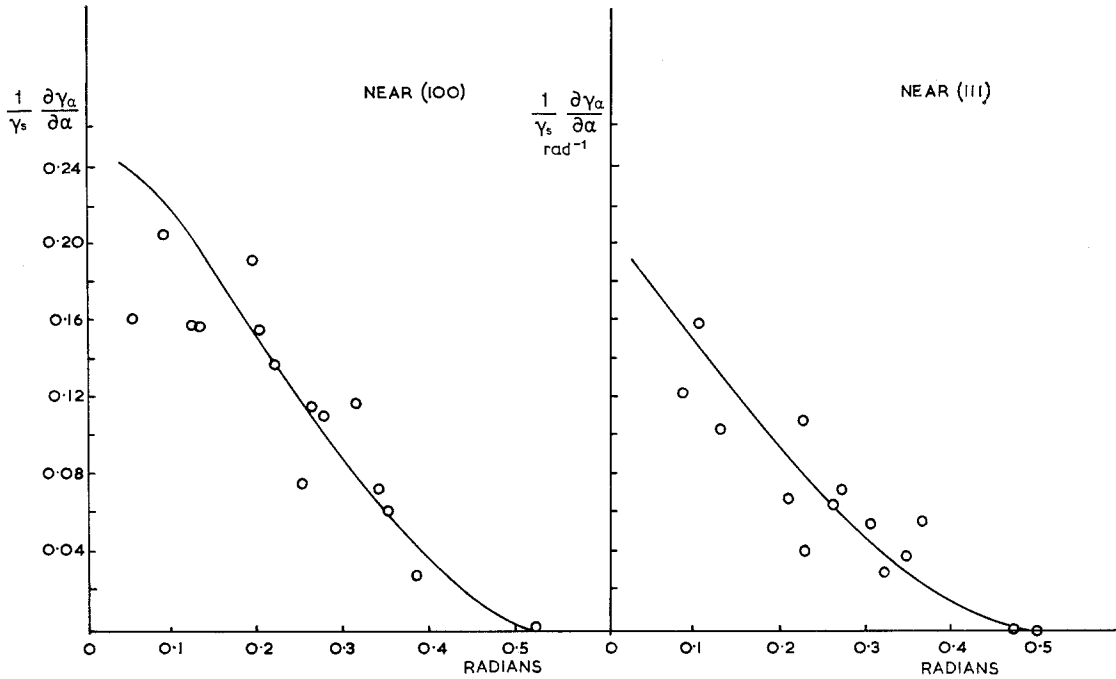


Figure 4 Torque terms  $(1/\gamma_s)(\partial\gamma/\partial\alpha)$  for nickel surfaces near (100) and near (111).

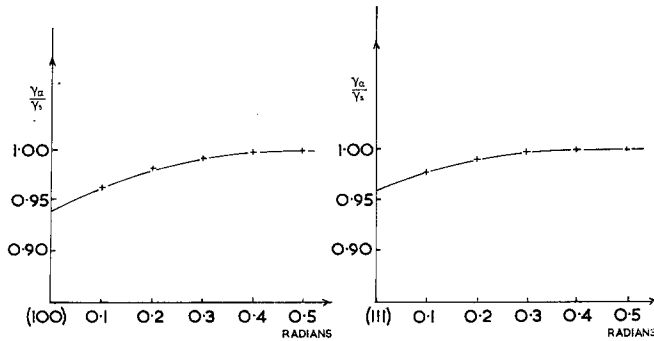


Figure 5 Surface energy anisotropy obtained by integration of Fig. 4. Ratio of energy of surface with orientation  $\alpha$  to average surface energy plotted versus orientation  $\alpha$ , for surfaces near (100) and near (111).

boundary energy with misorientation across the boundary, but part will be due to errors caused by the assumption that the boundary is perpendicular to the free surface, and part due to residual torque-term errors introduced by the simplifying assumptions of the torque-term analysis. The difference between the means of the corrected and the uncorrected  $\gamma_B/\gamma_s$  values is less than the possible error of either mean. Thus the common assumption, that the torque terms can be neglected when average values of large numbers of grain-boundary measurements are considered, is sufficiently justified in this case.

We have examined the misorientation of those boundaries in Fig. 7b that have  $\gamma_B/\gamma_s$  values below 0.30, to see how the grain-boundary energy correlates with misorientation. As is well known, there are twenty-four different ways in which the misorientation of two cubic crystals can be described in terms of one single rotation. It is usual to take the smallest of the twenty-four rotation angles to describe the misorientation; the expected distribution of this angle for randomly-oriented grains is also known [5]. However, we have found no significant correlation between the measured grain-boundary

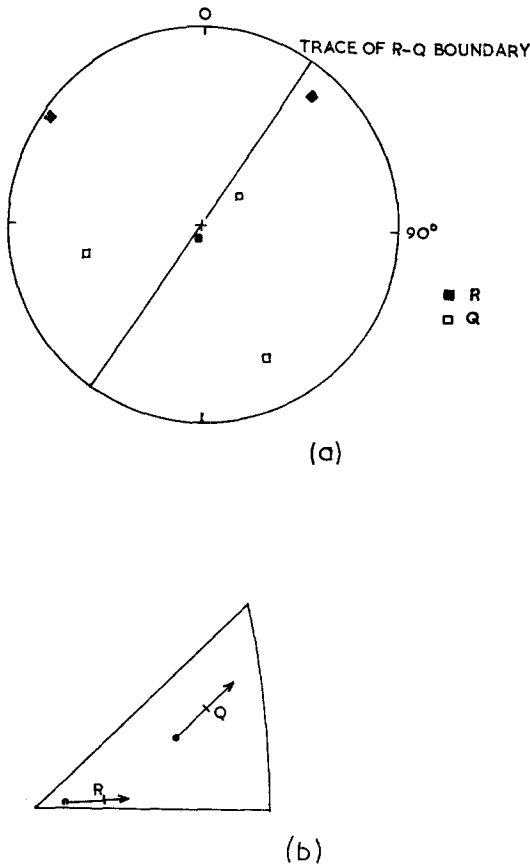


Figure 6 Orientation of two grains forming a typical boundary R-Q having an apparent  $\gamma_B/\gamma_S$  of 0.284: (a) Stereogram, showing the {100} poles and the trace of the boundary. (b) Unit triangle. The base of the arrows give the grain-surface orientations; the lines across the arrows give the orientations at the groove root. Surface orientations at groove root give surface torque terms  $(1/\gamma_S)(\partial\gamma_R/\partial\theta_R) = -0.12$  and  $(1/\gamma_S)(\partial\gamma_Q/\partial\theta_Q) = 0.022$ , so the corrected value of  $\gamma_B/\gamma_S$  for R-Q is 0.382.

energy and the smallest misorientation angle for the boundaries we have examined. Further work on this is necessary: it may be that the description of the boundary in terms of the minimum dislocation content required for the misorientation will make apparent a relation with boundary energy which the use of a single rotation angle does not show.

In this investigation, no boundaries (other than twin boundaries) were seen to be not flat on a microscopic scale. (Twin boundaries of course were generally faceted, i.e., broken up into coherent and noncoherent boundary regions.) However, most of the boundaries had some

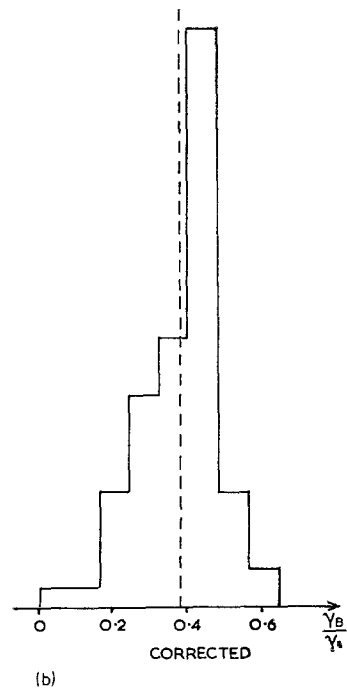
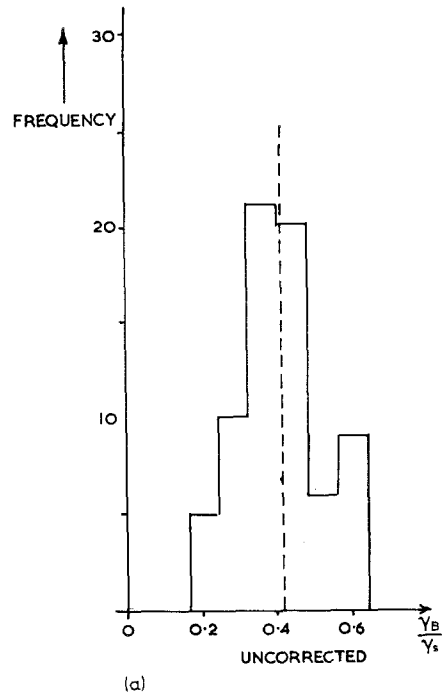


Figure 7 (a) Histogram for uncorrected values of  $\gamma_B/\gamma_S$ ; Mean value of  $\gamma_B/\gamma_S$  is 0.41 ( $\pm 0.04$ ). (b) Histogram for corrected values of  $\gamma_B/\gamma_S$ ; Mean value of  $\gamma_B/\gamma_S$  is 0.38 ( $\pm 0.05$ ).

curvature, in the plane of the surface, due to constraints at grain-boundary junctions. In such cases there was no significant variation in grain-boundary energy with boundary orientation for a fixed misorientation across the boundary.

It is worth comparing the torque terms and  $\gamma$ -plot described in this paper with the earlier measurement of a  $\gamma$ -plot for nickel [4], using the same technique and material of similar purity. The present  $\gamma$ -plot is similar to the earlier one, though somewhat shallower. The (100) cusp is still the most prominent (0.94 against 0.92) and the (111) cusp is effectively unchanged (0.96). The difference is probably due to the better vacuum now available ( $5 \times 10^{-7}$  Torr against  $\sim 10^{-5}$  Torr). However, there is good reason to believe that we are not dealing with a clean nickel surface; nickel of similar purity heated in an ultra-high-vacuum system (better than  $10^{-9}$  Torr) fitted with Auger analysis facilities has shown a fairly rapid build-up of sulphur on the nickel surface during heating.

For the purpose of measuring grain-boundary energies, the surface contamination is probably acceptable. The surface energy acts only as an internal reference standard. Provided the surface condition is the same during the set of measurements, the  $\gamma_s$  value is a constant that cancels out when deriving the final  $\gamma_b$  result.

The polycrystalline-sheet specimens used in these experiments make it difficult to check on boundary curvature perpendicular to the specimen surface and this introduces the possible errors due to non-normal boundary orientation at the surface. From this point of view, the method

due to M. McLean [6, 7] which used individual grain boundaries in a wire with a "bamboo" structure, has considerable advantage for this type of experiment. In McLean's method, the specimen is smaller, and each crystal is constrained only by two boundaries, so the approach to equilibrium by diffusional processes is much more rapid. Also grains in such a wire specimen have more freedom to change their orientation during equilibration by the movement of dislocations from one boundary to the other, than do grains in a polycrystalline sheet specimen. This technique does however require the sophisticated method of analysis described by McLean and Gale [6].

### Acknowledgement

This work was supported in part by the AERE, Harwell under contract EMR.2033.

### References

1. E. D. HONDROS, in "Interfaces - Conference Proceedings", ed. R. C. Gifkins (Butterworths, Sydney, 1969).
2. C. HERRING in "The Physics of Powder Metallurgy", ed. W. E. Kingston (McGraw-Hill, New York, 1951).
3. H. MYKURA, *Bull. Inst. Met.* **4** (1958) 102.
4. *Idem*, *Acta Metallurgica* **9** (1961) 570.
5. D. C. HANDSCOMB, *Canad. J. Math.* **10** (1958) 85.
6. M. MCLEAN and B. GALE, *Phil. Mag.* **20** (1969) 1033.
7. M. MCLEAN, *J. Mater. Sci.* **8** (1973) April issue.

Received 11 August and accepted 30 October 1972.